THE ASTROPHYSICAL JOURNAL, 252:524–528, 1982 January 15

COLLAPSE MODELS FOR DARK INTERSTELLAR CLOUDS

KAREN R. VILLERE
Board of Studies in Astronomy and Astrophysics, University of California, Santa Cruz, and Space Science Division, NASA Ames Research Center, Moffett Field, California

AND

DAVID C. BLACK
Space Science Division, NASA Ames Research Center, Moffett Field, California
Received 1981 January 6; accepted 1981 August 24

ABSTRACT

Properties of self-consistent numerical hydrodynamic models are compared with observed properties of several dark clouds. The results are consistent with the view that these clouds are undergoing gravitational collapse. The clouds appear to have evolved from similar initial states and to have ages comparable to their free-fall times. Derived cloud masses range between 10 and 10^3 $M_\odot$, correlating with cloud size. The models reproduce observed cloud-to-cloud variations in the ^{13}CO abundance, and they offer additional evidence that the ^{13}CO abundance varies within individual clouds.

Subject headings: hydrodynamics — nebulae: general

I. INTRODUCTION

Dark interstellar clouds have received considerable recent attention because of increasing evidence that they are undergoing collapse. These objects range in size from globules smaller than a parsec to giant clouds of 10 parsecs or more. We may ask whether this diversity in size reflects other fundamental differences. Do the clouds differ merely in scale, or do they have different origins and different dynamical and chemical evolution?

One approach to answering such questions is to compare observed properties of the clouds with self-consistent numerical hydrodynamic models. The largest clouds have a complex structure that is not easily represented with current numerical techniques, but several globules have been modeled by Villere and Black (1980, Paper I). In this paper we extend the cloud-model comparison to configurations intermediate in size between the globules and the giant clouds. Twelve clouds are discussed: the five clouds modeled in Paper I (ORI-I-2, B68, B163, B163SW, and B335), one cloud (B361) which could not be modeled with the assumptions of Paper I, and six additional clouds (L1253, L1407, L1551, L134N, L1257, and L1235). There is an order of magnitude difference in size between the smallest of these objects (ORI-I-2) and the largest (L1235).

II. OBSERVATIONAL DATA

The numerical models are fitted to the following measured quantities: (1) $N_{13}(0)$, the ^{13}CO column density at the center of the cloud; (2) R_c, the core radius on the major axis, defined as the distance from the center of the cloud to the point at which the ^{13}CO column density is 50% of $N_{13}(0)$; (3) Z_c/R_c, the ratio of the minor-axis and major-axis core radii; (4) $V_{13}(0)$, the half-width at half-height of the ^{13}CO line profile at the cloud center; (5) $V_{\rm rot}(R_c)$, the rotational velocity at

TABLE 1

OBSERVED PROPERTIES OF DARK CLOUDS

Parameter	L1253	L1407	L1551	L134N	L1257	L1235
$N_{13}(0)$ (cm^{-2})[a]	9.0E15	1.5E16	6.6E15	1.2E16	1.3E16	1.1E16
R_c (cm)[a]	6.1E17	8.2E17	1.3E18	1.6E18	1.9E18	3.3E18
Z_c/R_c[a]	0.8	0.7	0.9	0.8	0.4	0.4
$V_{13}(0)$ (km s^{-1})[b]	0.85	1.20	0.70	0.95	1.25	0.9
$V_{\rm rot}(R_c)$ (km s^{-1})[a] ...	0.2	0	0	0	0.8	0.5
$R_{\rm opt}/R_c$[a]	0.7	1.5	1.1	0.8	1.1	1.0
Distance (pc)[a]	140	170	160	160	140	200

[a] Snell 1979.
[b] R. L. Snell, private communication.

the edge of the ^{13}CO core; and (6) R_{opt}/R_c, the ratio of the optical radius, measured on a red Palomar Sky Survey print, to the ^{13}CO core radius. Our analysis is restricted to clouds sufficiently regular in shape that the above parameters are well defined. Measured values of the fitting parameters and distances for the six new clouds are given in Table 1.

III. MODEL-FITTING TECHNIQUE

The present study follows the procedure discussed in Paper I. Sequences of models were constructed with the Black-Bodenheimer (1975) hydrodynamic code, starting from spherical configurations of uniform temperature, density, and angular velocity. A particular sequence is defined by the total mass M, the *initial* ratio α of the thermal energy to the gravitational energy, and the *initial* ratio β of the rotational energy to the gravitational energy. Calculations were done for 17 combinations of α and β in the ranges $\alpha = 0.05$–1.6 and $\beta = 0$–0.32, and the numerical results were scaled to represent masses between 10 and 10^4 $M_\odot$. The general characteristics of the evolution and detailed characteristics of several sequences are described by Black and Bodenheimer (1976).

The fitting parameters are calculated from the models as functions of α, β, M, the inclination of the rotation axis, and the evolutionary time. Where appropriate, they are averaged over the model to represent observations with a finite-resolution telescope. The details of these calculations are described in Paper I. We emphasize that the model line widths derive solely from collapse and rotational motions (see § IV*e*).

Because the hydrodynamic code does not include molecular chemistry, spatial variation of the ^{13}CO abundance has been specified arbitrarily. In this work the parameters which depend on the ^{13}CO abundance are derived under two alternative assumptions:

Case A.—The volume density of ^{13}CO relative to that of H_2 is uniform throughout the model,

$$n(^{13}CO)/n(H_2) = c_A.$$

Case B.—The volume density of ^{13}CO relative to that of H_2 decreases at high density (as suggested by results in Paper I), according to the prescription

$$n(^{13}CO)/n(H_2) = c_B \quad \text{for } n(H_2) \le 10^3 \text{ cm}^{-3},$$

$$= \frac{c_B}{n(H_2)/10^3} \quad \text{for } n(H_2) > 10^3 \text{ cm}^{-3}.$$

Values of the constants c_A and c_B are derived for each cloud.

The best-fit model to each cloud is taken to be the model for which the mean-square relative error in the fitting parameters is a minimum. Best fits from Case A and Case B models will be presented separately.

IV. PROPERTIES OF THE BEST-FIT MODELS

Derived model parameters for the clouds not discussed in Paper I are listed in Table 2. These parameters are from the Case B models. Because the parameters to which the models are fitted have errors as large as 50%, due to uncertainty in the cloud distances and the finite spatial and velocity resolution of the CO observations, each cloud could be fitted with a large range of models, and the derived parameters have as much as an order of magnitude uncertainty (see Paper I, Table 2). We feel, therefore, that it is more meaningful to consider average properties of the cloud models and statistical correlations of parameters than to describe the detailed structure of individual models.

a) Evidence for Collapse

Each of the clouds studied here could be fitted only with models from sequences satisfying the Jeans condition for sustained collapse. Models from the sequences which violate this condition and undergo a bounce could not be fitted to one or more observed parameters. Our results are thus consistent with the notion that these clouds are collapsing toward higher density states.

Moreover, many of the clouds are best-fitted by sequences starting from initial models highly unstable to collapse ($\alpha \ll 1$). They apparently do not conform to the classic picture of gradually accelerated collapse from a

TABLE 2

PROPERTIES OF CASE B CLOUD MODELS

Cloud	α	β	$M/M_\odot$	$M/M_\odot$ within $A_v = 1$	i (deg)	t (yr)
L1257	0.16	0.08	240	130	15	2.8E6
L134N ...	0.5	0	910	72	...	5.2E7
L1235	0.16	0.08	330	190	15	3.9E6
L1551	0.16	0	120	115	...	1.0E6
L1407	0.05	0	190	190	...	2.8E5
L1253	0.5	0.08	19	18	60	1.3E6

configuration near the Jeans stability limit. The initial values of α and β inferred for these clouds are similar to the α and β values obtained by Bodenheimer and Boss (1982) for binary fragments in three-dimensional collapse calculations.

b) Dependence of Derived Parameters on Cloud Size

The mass, age, and initial values of α and β for the best-fit models are plotted in Figure 1 against the cloud size, as indicated by the ^{13}CO core radius R_c. The right-hand column of diagrams gives results for Case A models; the left-hand column gives results for Case B. Fewer points are plotted in the Case A diagrams because the clouds B361 and L1257 could not be fitted with Case A models. The solid line in each diagram is a least-squares fit to the variation of the model parameter with R_c. Also shown is the value of the correlation coefficient r. A correlation is considered significant if $|r|>0.5$ and highly significant if $|r|>0.8$.

The following general relationships are evident in Figure 1:

1. There is a highly significant correlation between the total mass and the core size in Case B, and a marginally significant correlation in Case A. This is a comforting result, as we expect the larger clouds to be more massive. The masses range between 10 and 10^3 $M_\odot$, increasing approximately as R_c^2 in Case B, and as R_c in Case A. Masses for smaller clouds (globules) are on average 3 times larger from Case A models than from Case B. It should be emphasized that the quantity plotted is the total mass—not the core mass. For most of these models, a core of radius R_c contains between 40% and 90% of the total mass.

2. The clouds seem to be at similar stages of evolution. Although there is some suggestion in Case A that the age relative to the free-fall time, $t/t_{\rm ff}$ is an increasing function of R_c, there is no correlation between the relative age and the cloud size in Case B. The mean value and standard deviation of $t/t_{\rm ff}$ for all clouds is 0.85 ± 0.23 in Case A and 1.00 ± 0.21 in Case B. Thus each cloud seems to have evolved for approximately one free-fall time. The absolute age, however, is not the same for all clouds because $t_{\rm ff}$ is proportional to the mass. The absolute ages range between 10^5 and 5×10^7 years.

We are led to speculate that a cloud collapses for approximately one free-fall time and then fragments or in some other way changes form so as to no longer resemble objects of the type modeled here. Perhaps the irregularly shaped clouds have undergone this transformation.

3. There is no significant correlation between the *initial* values of α or β and the cloud size in either Case A or Case B. It is difficult to say whether there is an intrinsic range of α and β at each value of R_c because the uncertainty in the values is comparable to the scatter about the mean curve, but the average initial conditions appear to be uniform over the range of clouds studied. The mean value and standard deviation of α is 0.18 ± 0.17 in Case A and 0.25 ± 0.18 in Case B. The corresponding values for β are 0.10 ± 0.12 and 0.06 ± 0.09.

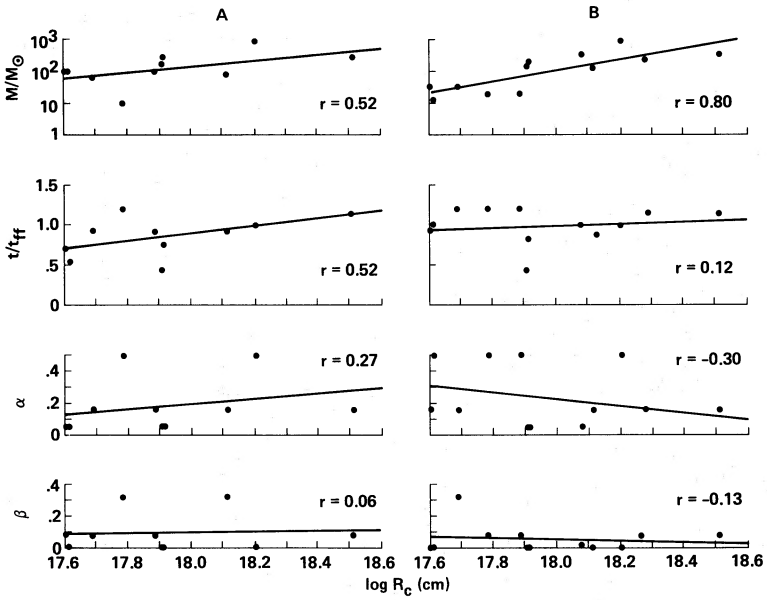

FIG. 1.—Dependence of derived parameters on cloud size. Total mass, relative age, and initial α and β are plotted vs. the ^{13}CO core size.

c) *The* $^{13}CO/H_2$ *Ratio*

The relative distribution of molecular species is not easily observed in the small clouds considered here. Available measurements give average abundance variations from cloud to cloud rather than detailed variations within individual clouds. The situation is further complicated because the abundance of molecular hydrogen must be inferred from observation of other molecules, and the interpretation of any molecular line measurement requires a model of the overall structure of the cloud.

In Figure 2, the density variation of the ^{13}CO abundance from two observational studies is compared with variations predicted by our models. The column density ratio $N(^{13}CO)/N(H_2)$ is plotted against the gas density $n(H_2)$. Values from the models are averaged over a 2′ diameter core, and results from Case A and Case B models are shown on separate diagrams. Also shown, and repeated on each diagram, are values obtained by Wootten *et al.* (1978) and Snell (1979) from H_2CO and CO observations of a variety of dense clouds, interpreted with simple models of constant temperature, density, and molecular abundance. A direct comparison of the models and the observations is not possible because the three sets of data refer to different cloud positions or to entirely different clouds. Nevertheless, all the data clearly show the same general *tendency* toward a correlated decrease in ^{13}CO abundance with an increase in gas density. This trend, which we pointed out for the globules in Paper I, apparently extends to the larger clouds as well.

Unfortunately, Figure 2 provides little basis for distinguishing between the alternatives of: a uniform ^{13}CO abundance in each cloud with variations from cloud to cloud (Case A), and an abundance that varies *within* individual clouds (Case B). The mean slope and the scatter of points is approximately the same for our Case A models, our Case B models, and the models of the other authors. There is, however, additional evidence from our model fitting that favors Case B. Two clouds (B361 and L1257) could not be fitted with the Case A models, but could be fitted with Case B models. Also, for each of the other clouds, the fit to the ^{13}CO line width was better with models of Case B. Finally, values derived from Case B models for the constant c_B, which determines the $^{13}CO/H_2$ ratio at low density, are close to the value of 2×10^{-6} measured in low density clouds by Dickman (1978). The average value of c_B for our 12 Case B cloud models is 2.5 $(\pm1.5)\times10^{-6}$, with no systematic dependence on $n(H_2)$.

d) *Total Mass*

The total masses derived from our models of individual clouds exceed previous mass estimates for these systems. For example, the masses given in Table 2 are

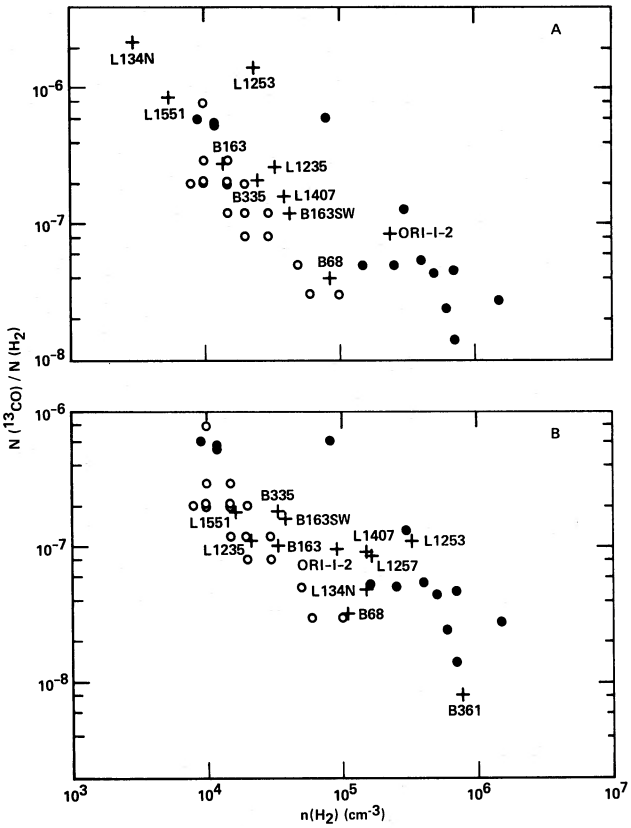

FIG. 2.—Column density ratio $N(^{13}CO)/N(H_2)$ vs. total gas density in a variety of interstellar clouds. The plus signs are our best-fit Case A and Case B models. Filled circles are measurements by Wootten *et al.* (1978). Open circles are measurements by Snell (1979).

2–10 times higher than those given by Snell (1979). Three factors could readily account for this apparent discrepancy.

First, a substantial fraction (~0.5–0.9) of the mass in our models of the three largest clouds (L1235, L134N, and L1257) would not be detectable by means of ^{13}CO observations. That is, the ^{13}CO column density for these regions of the model falls below the minimum density measured by Snell. We note that if we consider just the mass with $A_v \geq 1$ mag (Table 2), which is comparable to the mass that would be detectable in ^{13}CO, our model masses are much closer to those inferred by the observers. The second factor which influences model masses is the $n(^{13}CO)/n(H_2)$ ratio. Snell and others use their observationally determined ^{13}CO abundance and an *assumed* $n(^{13}CO)/n(H_2)$ ratio to estimate the cloud (i.e., H_2) mass. Most such estimates assume that this ratio is 2×10^{-6}. However, as this work and the work of Snell and of Wootten *et al.* show, the average $n(^{13}CO)/n(H_2)$ ratio in the clouds in question is a factor of 3–10 smaller than the value 2×10^{-6}. Thus,

published mass estimates using ^{13}CO observations should be considered as lower limits which are consistent with the masses obtained in this study. The third factor pertains to estimates of the mass of the smaller clouds considered in our study, estimates based on optical absorption data (Bok, Cordwell, and Cromwell 1971; Bok and McCarthy 1974; Schmidt 1975). Combining the minimum optical absorption with an assumed gas/dust mass ratio (typically ~ 100), one obtains a *lower* limit to the total mass of a cloud. Our models of the Bok globules have more mass (i.e., greater optical absorption) in the dense inner regions where the underestimate of optical absorption by the observers would be significant. It is worth noting that our model of B335 is consistent with the dust mass estimated for the core of this cloud from far-infrared emission (Keene *et al.* 1980) if the gas/dust ratio is 150. We conclude that while the masses obtained from self-consistent dynamic models of these clouds are higher than the mass estimates given by previous workers, the earlier estimates are lower limits, and in this regard they are consistent with the masses of the models.

e) Sensitivity to Model Line Widths

The line width appropriate to each model is estimated from the line-of-sight velocity (see Appendix A, Paper I). A preliminary comparison with detailed line profiles for several representative models (to be presented in a forthcoming paper) shows the estimated widths to be accurate to within a factor of 2. To test the sensitivity of derived parameters to uncertainty in the line width, the cloud fitting was repeated with all model line widths increased by a factor of 2. This test also shows qualitatively the effects of additional line broadening mechanisms, such as turbulence. The increased line width produced average changes of 50% in the parameters α, β, M, and t and an average factor of 2 change in the ratio $n(^{13}CO)/n(H_2)$. The only systematic trends were toward smaller age and larger $n(^{13}CO)/n(H_2)$. However, there were no qualitative changes in the cloud properties and correlations discussed above. Our general conclusions regarding the clouds' structure and evolutionary state are thus valid over a reasonable range in uncertainty of the individual line widths.

V. CONCLUSIONS

Our cloud-model comparisons suggest that dark clouds with an order of magnitude range in size form a homogeneous class, differing only in mass and scale. The clouds considered here could be fitted only with models which are gravitationally unstable and undergoing collapse. They appear to have started from similar initial states and to be observed at comparable stages of evolution. The inclusion of molecular abundance gradients affects individual derived parameters but not our general conclusions about the nature of the clouds.

We emphasize that because of both observational and modeling uncertainties this study has concentrated on considerations of general properties and trends of cloud parameters, rather than on detailed characteristics of individual clouds. Moreover, we have considered only a limited range of models. Models with initial conditions which differ significantly from those used in this study, or models that include other physical effects (such as turbulence or magnetic fields), might also agree with the observations and might predict different structure and history for the clouds. It is hoped that the present work will be an impetus for further modeling efforts and for more extensive and higher resolution observations.

We thank Ronald Snell for communicating unpublished data and an anonymous referee for helpful suggestions. Funds for the support of this study have been allocated by the NASA Ames Research Center, Moffett Field, California, under Interchange No. NCA2-OR690-001.

REFERENCES

Black, D. C., and Bodenheimer, P. 1975, *Ap. J.*, **199**, 619.
_____. 1976, *Ap. J.*, **206**, 138.
Bodenheimer, P., and Boss, A. P. 1982, *Ap. J.*, submitted.
Bok, B. J., Cordwell, C. S., and Cromwell, R. H. 1971, in *Dark Nebulae, Globules, and Protostars*, ed. B. T. Lynds (Tucson: University of Arizona Press), p. 33.
Bok, B. J., and McCarthy, C. C. 1974, *A.J.*, **79**, 42.
Dickman, R. L. 1978, *Ap. J. Suppl.*, **37**, 407.
Keene, J., Harper, D. A., Hildebrand, R. H., and Whitcomb, S. E. 1980, *Ap. J. (Letters)*, **240**, L43.
Schmidt, E. G. 1975, *M.N.R.A.S.*, **172**, 401.
Snell, R. L. 1979, Ph.D. thesis, University of Texas, Austin.
Villere, K. R., and Black, D. C. 1980, *Ap. J.*, **236**, 192 (Paper I).
Wootten, A., Evans, N. J., Snell, R., and Vanden Bout, P. 1978, *Ap. J. (Letters)*, **225**, L143.

DAVID C. BLACK and KAREN R. VILLERE: Space Science Division, MS 245-3, NASA Ames Research Center, Moffett Field, CA 94035